Bioanalysis

ISSN: (Print) (Online) Journal homepage: www.tandfonline.com/journals/ibio20

Comparative pharmacokinetic study of Anisodamine Hydrobromide tablets and injection in septic acute lung injury rats

Rui Wu, Fang Zhang, Yanfang Liu, Yujie Yu, Jianlan Zhang, Chenhao Yao, Shu Dai, Feng Wan, Feng Nan & Yunxia Li

To cite this article: Rui Wu, Fang Zhang, Yanfang Liu, Yujie Yu, Jianlan Zhang, Chenhao Yao, Shu Dai, Feng Wan, Feng Nan & Yunxia Li (08 Aug 2024): Comparative pharmacokinetic study of Anisodamine Hydrobromide tablets and injection in septic acute lung injury rats, Bioanalysis, DOI: 10.1080/17576180.2024.2383106

To link to this article: https://doi.org/10.1080/17576180.2024.2383106

Published online: 08 Aug 2024.

BIOANALYSIS
https://doi.org/10.1080/17576180.2024.2383106

Taylor & Francis
Taylor & Francis Group

RESEARCH ARTICLE

Comparative pharmacokinetic study of Anisodamine Hydrobromide tablets and injection in septic acute lung injury rats

Rui Wu[a], Fang Zhang[a], Yanfang Liu[a], Yujie Yu[a], Jianlan Zhang[a], Chenhao Yao[a], Shu Dai[a], Feng Wan[a,b], Feng Nan[*,c] and Yunxia Li[**,a]

[a]State Key Laboratory of Southwestern Chinese Medicine Resources, Key Laboratory of Standardization for Chinese Herbal Medicine, Ministry of Education, School of Pharmacy, Chengdu University of Traditional Chinese Medicine, Chengdu, 611137, China; [b]Chengdu NO. 1 Pharmaceutical Co., Ltd., Pengzhou, Sichuan, 610031, China; [c]Drug Clinical Trial Institution, The Affiliated Hospital of Chengdu University of Traditional Chinese Medicine, Chengdu, Sichuan, 610075, China

ABSTRACT

Aim: We aimed to establish a sensitive LC-MS/MS method to analyze the pharmacokinetics of Ani HBr tablets and injection. **Methods:** Around 10 mmNH_4Ac containing 0.1% formic acid and acetonitrile were used as the mobile phase. Acute lung injury in septic and normal rats, respectively, were administered Ani HBr tablets at doses of 12.5, 25 and 50 mg/kg and injection at doses of 4, 8 and 16 mg/kg, followed by extraction of the drugs from plasma using ethyl acetate for subsequent analysis. **Results & conclusion:** The method met the requirements for biological analysis. Ani HBr tablets absorbed slowly in rats with disease, tail vein administration was a more promising approach for treating septic acute lung injury.

ARTICLE HISTORY
Received 21 March 2024
Accepted 18 July 2024

KEYWORDS
Anisodamine hydrobromide; LC-MS/MS; pharmacokinetics; septic acute lung injury

1. Introduction

Sepsis is an acute multiorgan dysfunction syndrome caused by infection leading to excessive systemic inflammation and immunosuppression [1,2]. There were approximately 49 million cases of sepsis globally and approximately 11 million sepsis-related deaths from 1990 to 2017, accounting for 20% of global deaths. More notably, sepsis exists in Asia with the highest incidence and mortality [3]. Lung is the most vulnerable organ in sepsis, and the inflammatory cascade caused by it will cause acute lung injury (ALI) [2].

Anisodamine hydrobromide (Ani HBr) (Figure 1A) is a natural L-alkaloid hydrobromide extracted from *Anisodus tanguticus* (Maxim.) Pascher, a unique plant from the Solanaceae in western China . Ani HBr improves lipopolysaccharides (LPS)-induced septic ALI in rats through multiple pathways, such as anti-apoptotic, anti-oxidant stress and anti-inflammatory effects [4,5]. In addition, Ani HBr reduces vascular microcirculation disorders caused by sepsis, stabilizing the permeability of cell membranes and endothelial cells, to effectively improve hemodynamics and avoid organ hypoxia and even functional failure [6,7]. Based on extensive preclinical pharmacological mechanism, it has been applied for the treatment of septic shock and microcirculation disorders in patients with abdominal pain in clinical practice [8–10]. More importantly, Ani HBr significantly alleviates the symptoms of rapid breathing and increased blood oxygen saturation in patients infected with COVID-19 in 2019 [11]. Therefore, Ani HBr holds significant clinical implications and demonstrates broad potential for application in various medical fields.

The operation characteristics of medicines *in vivo* are intricately linked to their clinical application. Understanding the absorption and metabolism processes will offer valuable insights for determining optimal clinical dosages and frequencies for their administration. Furthermore, given the alterations in biofilm permeability during pathological states, the metabolic pathways of drugs may also exhibit variations. Consequently, investigating the medicine transport mechanism during disease conditions assumes even greater urgency [12,13]. Currently, however, there is a dearth of pharmacokinetic reports on Ani HBr. Thus, this study developed the LC-MS/MS method for it. For the first time, we explored the pharmacokinetic features of Ani HBr in rats across various administration routes, multiple doses and different physiological states, offering insights for clinical drug using.

2. Materials & methods

2.1. Chemicals & reagents

Anisodamine hydrochloride tablets with 5 mg/tablet and injection with 10 mg/ml were provided by Chengdu First Pharmaceutical Co., Ltd (Sichuan, China). Aniso-

CONTACT Feng Nan nanfeng0525@foxmail.com; Yunxia Li lyxtgyxcdutcm@163.com

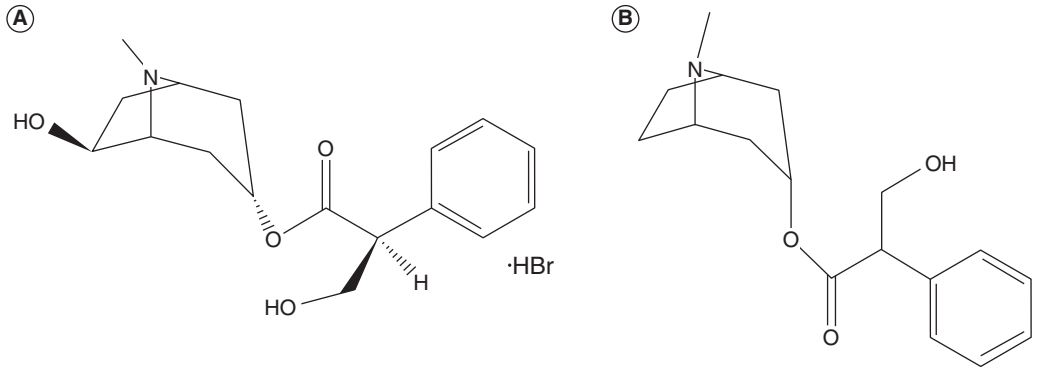

Figure 1. The chemical structures of Ani HBr **(A)** and IS **(B)**.

damine hydrochloride (purity ≥99.3%, batch:100051-201607) and atropine sulfate (internal standard, IS, purity ≥96.7%, batch: 10040-201613) were purchased from the National Institutes for Food and Drug Control (Beijing, China). Analytical-grade sodium hydroxide and ammonium acetate were obtained from Chengdu Kelong Chemical Co., Ltd (Sichuan, China). LPS (*Escherichia coli* O55:B5 L2880) was purchased from Sigma-Aldrich (St Louis, MO, USA).

Acetonitrile and ethyl acetate (HPLC-grade) was purchased from Fisher Scientific (Emerson, IA, USA). HPLC-grade formic acid was purchased from ACS Enko Chemical (China) Co., Ltd. The re-distilled water used throughout the analysis process in the laboratory was provided by an SZ-93 automatic double pure water distiller (Shanghai, China).

2.2. Establishment & evaluation of ALI animal model

Healthy Sprague-Dawley (SD) rats, an equal number of males and females, weighing 230–250 g were procured from Chengdu Dashuo Experimental Animal Co., Ltd. (Sichuan, China) and acclimatized for one week under a controlled environment with a 12-h light-dark cycle at 25°C and 75% relative humidity. During the adaptive feeding period, rats were allowed free access to food and water, with only fasting for 12 h prior to the experiment. All animal experiments in the project were followed the animal experiment protocol and guidelines approved by the Animal Experiment Theory Committee of Chengdu University of Traditional Chinese Medicine (No. TCM-2022-305).

We selected a cohort of healthy male and female SD rats and administered an intraperitoneal injection of LPS solution (10 mg/kg). After 3 h, we harvested the right lower lobe of the lung for Hematoxylin and eosin (HE) staining and weighed the left lung weight to compare the wet/dry weight ratio. After the lower lobe of the right lung was fixed in 4% paraformaldehyde for 48 h, paraffin embedded sections were made and stained. The evaluation criteria of ALI model were disruption of alveolar and interstitial structure, hemorrhage, neutrophil infiltration and serous exudation. The left lung of rats was also wet weighted and then dried in a constant temperature oven at 80°C for 24 h, the ratio of wet/dry weight of the left lung was calculated to evaluate the degree of pulmonary edema.

2.3. The methods for pretreatment of samples

The rat plasma sample (50 μl) was combined with IS working solution (25 μl), followed by the addition of 2 mol/l NaOH solution (10 μl). After adding 600 μl of ethyl acetate, the mixture was thoroughly mixed. Following centrifugation at 14,000 rpm for 5 min at 4°C, the supernatant (400 μl) was collected and subsequently evaporated under a stream of nitrogen in a water bath maintained at 40°C. Finally, the residues were re-dissolved in 50 μl of mobile phase and centrifuged at 14,000 rpm for 5 min at 4°C. Then, 40 μl of the supernatant was taken for sample loading and 10 μl was injected for analysis.

2.4. Preparation of standard solutions

Stock standard solution at 1.0 mg/ml for Ani HBr and was prepared with acetonitrile. Additionally, stock standard solution at 0.5 mg/ml for IS was prepared with methanol. IS working solution (150 ng/ml) was obtained by diluting IS stock standard solution with 50% methanol-water.

2.5. LC-MS/MS conditions

This project used the Shimadzu LC-20 series HPLC system (Tokyo, Japan) and AB Sciex 4000 Q TRAP (AB Sciex, Foster City, CA, USA) triple quadrupole mass spectrometer in series for LC-MS/MS analysis. The elution procedure was performed on a Phenomenex C_{18} column (3.0 × 50 mm, 5 μm), equipped with a pre-column (4 × 3.0 mm, 5 μm). The mobile phase A was 10 mmol/l

ammonium acetate containing 0.1% formic acid, and the mobile phase B was acetonitrile. Isometric elution was performed at 0.4 ml/min (1/9, v/v), and the analysis time was 4 minutes. The temperature of the column temperature was maintained at 50°C, and the automatic injection chamber was at 15°C.

The mass spectrometry was selected electrospray ionization (ESI) source for multiple reaction monitoring (MRM) mode monitoring in positive ion mode. The ionization voltage was 5500 V, and the ion source temperature was at 500°C. Nitrogen was used as the dryer, the atomization gas was at 50 psi, the auxiliary heating gas was at 50 psi, the curtain air was at 20 psi and the spray collision gas mode was selected as medium mode. The mass-to-charge ratio (m/z) for the quantitative ion pair for Ani HBr was 306.2→140.2, additionally, IS had a m/z value of 290.2→124.2.

2.6. Method validation

2.6.1. Specificity

To assess the specificity, a mixture of rat plasma samples from six different sources was prepared and compared against blank plasma samples, standard solutions with blank plasma samples and plasma sample from normal rats after oral administration of Ani HBr 12.5 mg/kg at 1 h. The response of blank plasma samples should be less than 20% of Ani HBr and less than 5% of IS.

2.6.2. Calibration curve

A series of working solutions were prepared by diluting the Ani HBr stock solution with acetonitrile to obtain concentrations of 20,000, 16,000, 12,000, 6000, 3000, 1000, 100 and 40 ng/ml, respectively. 30 μl of each working solution was added to 570 μl of blank plasma to prepare standard plasma samples with concentrations of Ani HBr at 1000, 800, 600, 300, 150, 50, 5 and 2 ng/ml, respectively. The weighted least squares linear regression method ($1/x^2$) was used to plot the peak area (Ani HBr/IS) against the ratio of calibration standard concentration to calibration curve. The acceptable calibration curve should possess an r-value exceeding 0.99.

Ani HBr quality control (QC) working solution is prepared by diluting the stock solution with acetonitrile, with concentrations of 16,000, 6000, 100 and 40 ng/ml, respectively. Next, high-quality control (QH), medium-quality control (QM), low-quality control (QL) and lower limit of quantification (LLOQ) plasma samples of Ani HBr were prepared by adding 30 μl working solution at concentrations of 800, 300, 5 and 2 ng/ml, respectively to 570 μl blank plasma.

2.6.3. Accuracy & precision

The accuracy and precision of the analytical method were evaluated by evaluating three batches of QC samples for four concentrations with six replicates for Ani HBr over three consecutive working days. Accuracy was defined as (the measured value / the true value) ×100%, and precision was defined as the relative standard deviation (RSD) of measured values, which were deemed acceptable within a fluctuation range of ±15%.

2.6.4. Extraction recovery & matrix effect

To assess the extraction recovery of Ani HBr and IS, the peak area ratio of QH, QM and QL samples with six replicates with that of the same concentration analyte in working solutions were compared. To evaluate the matrix effect of Ani HBr and IS, the peak area ratio of the working solution with QH, QM and QL concentrations after processing blank plasma samples from 6 different sources was compared with the peak area ratio of the pure same concentration working solution. The coefficient of variation (CV%) of the normalized IS should fall within a range of ±15%.

2.6.5. Dilution integrity

The plasma samples were prepared at 9000 ng/ml, then followed by a tenfold dilution with blank plasma to generate six parallel preparations for evaluating the linearity of sample dilutions. The acceptability criteria for accuracy and precision were within ±15% deviation from theoretical values.

2.6.6. Stability

To evaluate the stability of plasma samples, we assessed the short-term stability (at room temperature, 25°C for 12 h) and post-processing stability (in an autosampler at 15°C for 24 h) by testing six parallel QH, QM and QL samples. Additionally, we examined freeze-thaw stability (three cycles within 1 week) and long-term stability (1 month frozen at -80°C). The accuracy of QC samples within ±15% of the theoretical value was considered acceptable.

2.7. Pharmacokinetic study

Seventy-two healthy SD rats were randomly allocated into two groups: the intragastric administration (i.g.) group and the tail intravenous injection (i.v.) group. The rats underwent a 12-h fasting period with adlibitum access to water prior to the experiment. The i.g. group was randomly divided into three dosage groups: low-dose (12.5 mg/kg), medium-dose (25 mg/kg) and high-dose (50 mg/kg). Each group was further randomized into model and normal subgroups with six rats in each sub-

group that has equal number of male and female rats. The i.v group was also randomly divided into three dosage groups: low-dose (4 mg/kg), medium-dose (8 mg/kg) and high-dose (16 mg/kg). Each group was further randomized into model and normal subgroups with six rats in each subgroup that has equal number of male and female rats.

Based on blood collection methods from relevant literature [14,15], approximately 0.3 ml of blood was collected from the orbital venous plexus at pre-dose and after administration at 2, 5, 15, 30, 60, 90, 120, 240, 360, 480, 600 and 1440 min. After each blood collection, the rats drank freely to ensure the balance of blood volume in the rats and prevent excessive blood loss. The blood samples were collected in eppendorf tubes containing sodium heparin as an anticoagulant and immediately stored on ice. The blood samples were centrifuged at 4500 rpm, 4°C for 10 min to obtain plasma, which was then stored at -80°C for subsequent LC-MS/MS analysis.

2.8. Statistical analysis

Data acquisition was implemented in Analyst software (Version 1.6.3, AB SCIEX). Pharmacokinetic parameters were calculated using a non-compartmental analysis (NCA) model fitted by the Winnonlin 8.3.5 software, and the values were expressed as mean ± SD. Data analysis was performed using Graphpad Prism 9.0 and SPSS 26.0. The pharmacokinetic parameters of the normal group and the model group were compared. If the data met the normal distribution and homogeneity of variance, independent sample t-tests were selected, otherwise non-parametric tests were selected. The p value less than 0.05 was considered statistically significant.

3. Results

3.1. Evaluation of the ALI Model

3.1.1. Histopathological analysis

LPS-induced septic ALI, as shown in Figure 2, exhibited neutrophil infiltration in the alveolar interstitium and collapse of the alveoli compared with the control group. Additionally, there was evidence of bleeding. It was indicated that the successful establishment of a rat model for ALI induced by LPS-sepsis.

3.1.2. Lung dry/wet weight ratio

The left lung wet/dry weight ratio of rats in the control group and the model group was shown in Table 1, which in the model group was significantly higher than that in the control group, with statistical significance ($p < 0.01$), indicating that the ALI in LPS-sepsis was successfully constructed. For subsequent experiments, a dosage of 10 mg/kg LPS was chosen as the modeling agent.

3.2. Optimization of LC-MS/MS conditions

The analysis method's sensitivity was enhanced by reoptimizing the conditions for both mass spectrometry detection and liquid chromatography. Firstly, quantitative ion pairs were optimized using MRM mode. Given that both Ani HBr and IS alkaloids containing N^+, opting for the positive ion mode would be more advantageous in terms of enhancing sensitivity of ion pairs. Both Ani HBr and IS exhibited $[M + H]^+$ mode in their parent ions, with Ani HBr displaying m/z 306.2 and IS exhibiting m/z 290.2. The product ion spectra scan, as depicted in Figure 3, illustrated that the fragment ion corresponding to Ani HBr had a m/z of 140.2, while the fragment ion for IS exhibited an m/z value of 124.2. Consequently, the quantitative ion pair for Ani HBr was represented by m/z 306.2→140.2, and IS was denoted by m/z 290.2→124.2. For optimization of chromatographic conditions, different types of mobile phases were tested. We investigated the impact of pure water, 0.1% formic acid, 5 mmol/l ammonium acetate and 10 mmol/l ammonium acetate containing 0.1% formic acid on sensitivity. Around 10 mmol/l ammonium acetate containing 0.1% formic acid was ultimately determined as mobile phase A, as it significantly enhanced the sensitivity of the analyte and improved peak shape.

3.3. Method validation

3.3.1. Specificity

The interference of blank plasma on the sensitivity of analyte in LLOQ samples was below 20%, meanwhile the interference on the sensitivity of IS was less than 5%. Furthermore, the retention time of the target compound in plasma samples obtained from normal rats orally administered with 12.5 mg/kg Ani HBr tablets for 60 min closely resembles that observed at LLOQ levels, as depicted in Figure 4. These findings affirmed the method's excellent selectivity.

3.3.2. Calibration curve

The calibration curve demonstrated linearity, with a regression coefficient (r) exceeding 0.99, indicating a linear correlation between the ratio of Ani HBr and IS peak areas and the analyte concentration in rat plasma within the range of 2–1000 ng/ml. The linear equation for Ani HBr was as follows: $y = 0.00361x + 0.00439$, $r = 0.9979$.

3.3.3. Accuracy & precision

Based on this analytical method, the accuracy and precision of three batches for QC samples, both intra-batch

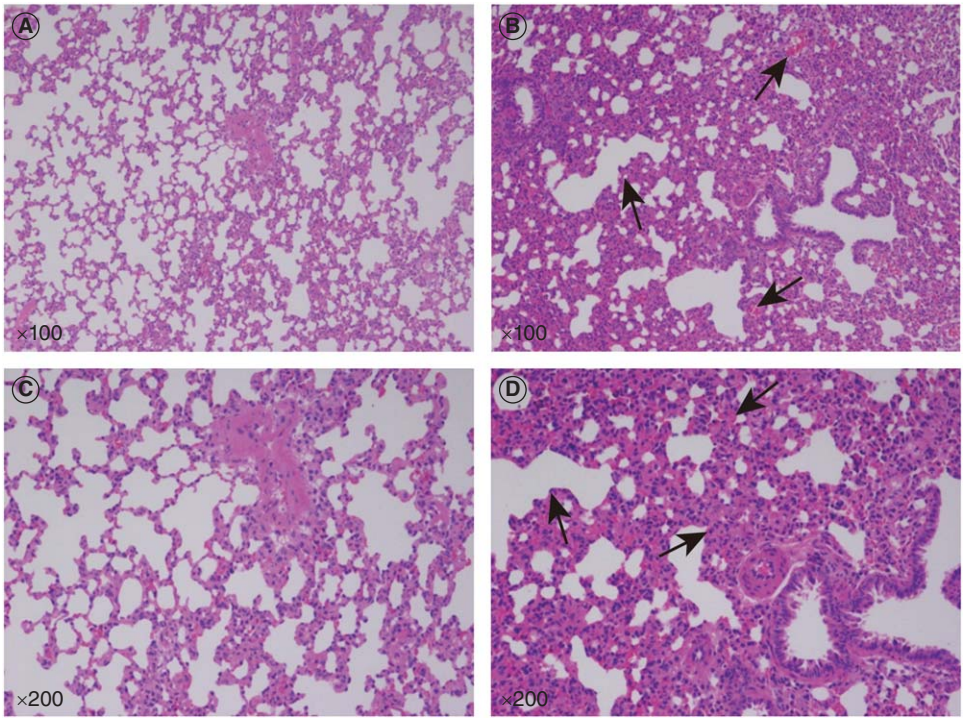

Figure 2. ALI in LPS-sepsis rats. **(A)** Control (×100). **(B)** 10 mg/kg LPS induced ALI (×100). **(C)** Control (×200). **(D)** 10 mg/kg LPS induced ALI (×200).

Table 1. The left Lung dry/wet weight ratio in rats (n = 6, mean ± SD).

Group	Lung dry/wet weight ratio
Control	5.00 ± 0.40
Model	6.64 ± 0.91[a]

[a]$p < 0.01$ compared with normal rats.
SD: Standard deviation.

and inter-batch were within the range of 85–115% of the theoretical concentration. As shown in Table 2, this indicated that the analytical method possessed reliable accuracy and precision.

3.3.4. Extraction recovery & matrix effect

The extraction recovery range of the analyte in QC samples was 89.51–91.87%, as presented in Table 3, with an RSD range of 3.63–10.19%. These results indicated a consistently stable extraction recovery rate for Ani HBr. Additionally, the matrix effects on the analytes were within an acceptable range, indicating that plasma matrix did not exert significant interference.

3.3.5. Dilution integrity

Given the potential for encountering biological specimens with concentrations surpassing the upper limit of quantification during actual testing, it is imperative to evaluate the reliability of dilution. Plasma samples with concentrations higher than upper limit of quantification were further diluted using blank plasma, with a dilution factor of 10. The accuracy of Ani HBr was determined to be 98.50%, with an RSD of 2.56%.

3.3.6. Stability

In this analytical method, the short-term stability, post-processing stability, freeze-thaw stability and long-term stability of QC samples were all examined. As shown in Table 4, the measured concentrations of QC samples under different conditions were within 15% of the theoretical concentration, with an RSD ranging from 2.31 to 11.16%, which met the requirements.

3.4. Pharmacokinetic study

To systematically investigate the pharmacokinetic characteristics of Ani HBr under physiological and pathological conditions, different doses and different administration routes, we evaluated the pharmacokinetic parameters of Ani HBr in normal and pathological rats after i.g. and i.v. of different doses. The mean plasma concentration-time profiles of rat were shown in Figure 5, and the pharmacokinetic parameters in Table 5.

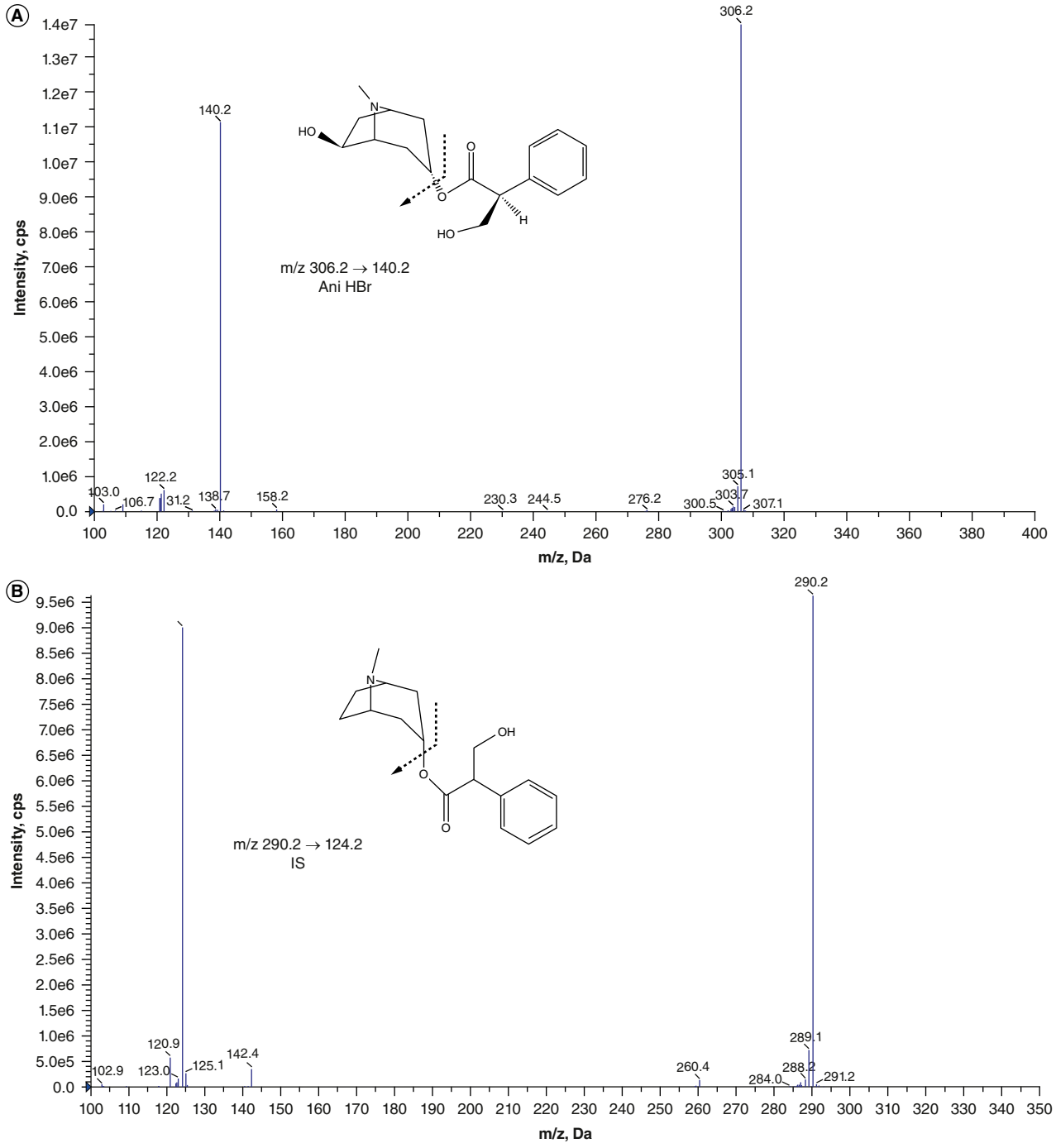

Figure 3. Product ion spectra (MS/MS) of **(A)** Ani HBr (m/z 306.2→140.2), **(B)** IS (m/z 290.2→124.2).

Under physiological conditions, following intragastric administration, the time to achieve the time to achieve maximum concentration (T_{max}) of Ani HBr tablets in rats across 12.5, 25 and 50 mg/kg was 12.5 ± 9.9, 6.7 ± 4.1 and 12.0 ± 10.4 min, respectively. This suggested a rapid absorption of Ani HBr under physiological conditions, allowing it to quickly enter the bloodstream and exert its effect, aligning with prior reports [16]. Moreover, the half-life of elimination ($T_{1/2}$) for Ani HBr in normal rats was about 3 h, which was also consistent with previous studies [16,17]. As the gavage dose increases, the maximum value of concentration (C_{max}) of rats after oral administration reached 164.5 ± 38.5, 364.0 ± 148.1 and 890.6 ± 313.9 ng/ml, demonstrating a dose-dependent effect. Furthermore, following i.v. of Ani HBr injection in rats, C_{max} rose in accordance with the dose, with values 1736.6 ± 453.5, 3550.0 ± 388.4 and 5750.0 ± 511.8 ng/ml. The aforementioned results indicated that, within the

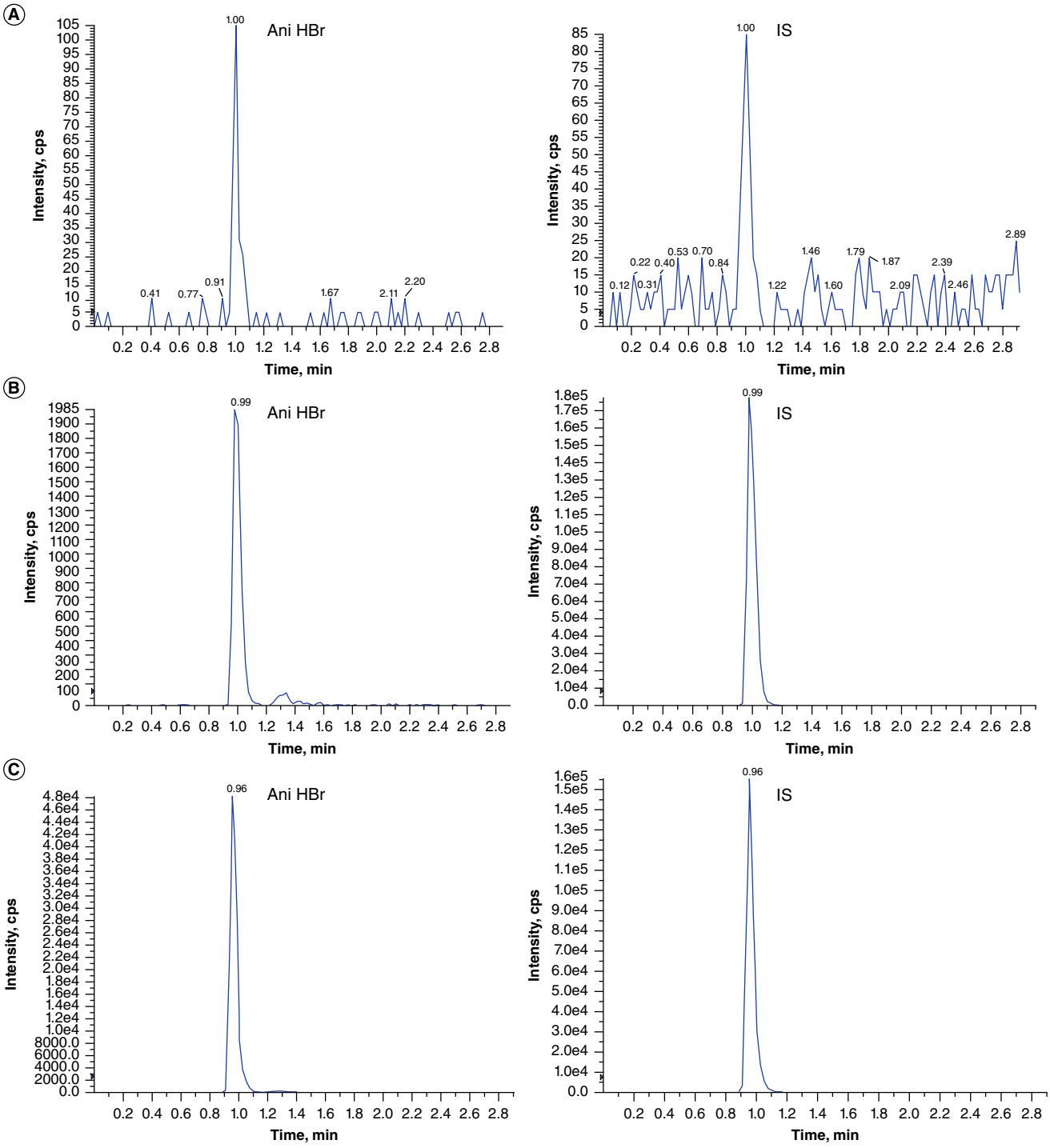

Figure 4. Representative chromatograms of Ani HBr and IS **(A)** blank plasma in rats, **(B)** LLOQ, **(C)** plasma from normal rats after oral administration of Ani HBr tablets 12.5 mg/kg at 60 min.

Table 2. Accuracy and precision for Ani HBr in rat plasma (n = 6).

Analyte	QC concentration (ng/ml)	Intra-batch		Inter-batch	
		Accuracy (%)	Precision (RSD, %)	Accuracy (%)	Precision (RSD, %)
Ani HBr	2	103.17	8.37	106.94	10.44
	5	105.13	6.98	107.14	10.29
	300	107.06	3.91	104.04	7.81
	800	101.58	4.38	98.00	5.72

Ani HBr: Anisodamine hydrochloride; QC: Quality control; RSD: Relative standard deviation.

Table 3. Extraction recovery and matrix effect for Ani HBr and IS in rat plasma (n = 6).

Analytes	QC concentration (ng/ml)	Extraction recovery		Matrix effect	
		Mean (%)	RSD (%)	Mean	CV (%)
Ani HBr	5	89.51	6.55	1.19	6.67
	300	91.87	10.19	1.07	6.77
	800	90.56	3.63	1.01	5.30
IS	150	88.52	4.03	0.96	3.85

Ani HBr: Anisodamine hydrochloride; CV: Coefficient of variation; IS: Internal standard; QC: Quality control; RSD: Relative standard deviation.

Table 4. Stability for Ani HBr in rat plasma (n = 6).

Analyte	QC concentration (ng/ml)	Short-term stability		Post-processing stability		Freeze-thaw stability		Long-term stability	
		Accuracy (%)	Precision (RSD, %)	Accuracy (%)	Precision (RSD, %)	Accuracy (%)	Precision (RSD, %)	Accuracy (%)	Precision (RSD, %)
Ani HBr	5	105.64	5.43	105.00	6.37	107.51	5.15	99.93	3.63
	300	106.71	6.90	107.33	2.81	108.20	11.16	107.13	3.31
	800	98.09	10.34	98.91	2.31	97.96	4.77	108.75	3.21

Ani HBr: Anisodamine hydrochloride; QC: Quality control; RSD: Relative standard deviation.

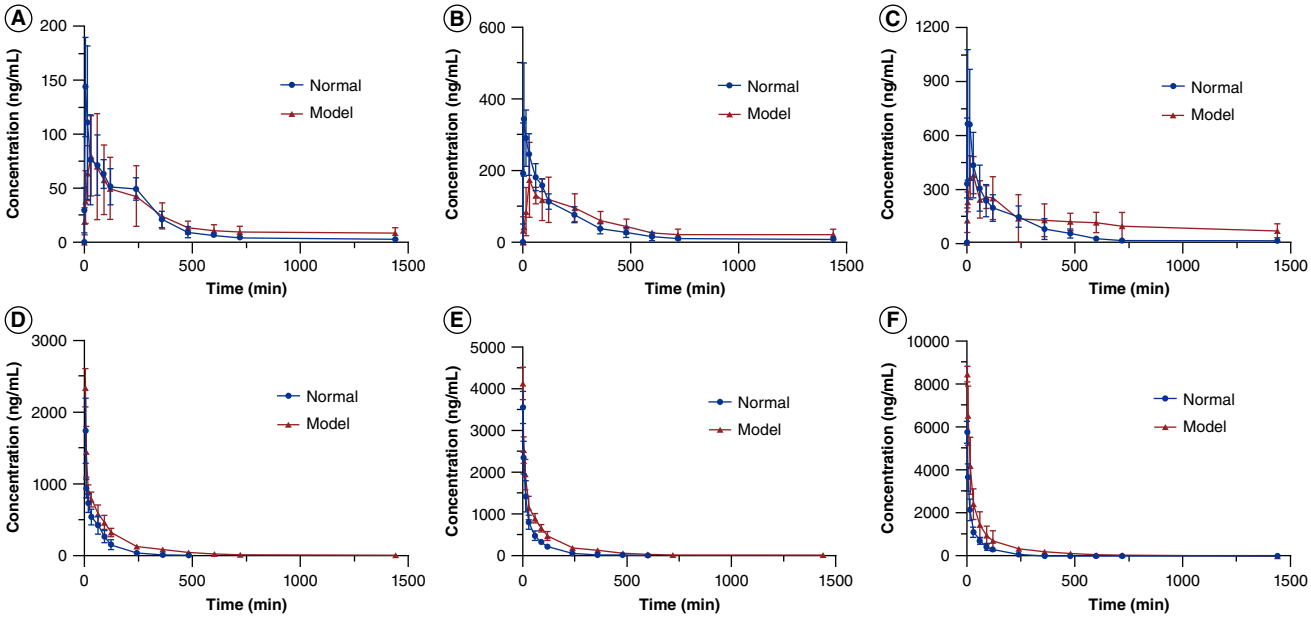

Figure 5. Mean plasma concentration-time profiles of normal and model rats after intragastric administration of 12.5 **(A)**, 25 **(B)** and 50 mg/kg **(C)** Ani HBr tablets, and after intravenous administration of 4 **(D)**, 8 **(E)** and 16 mg/kg **(F)** Ani HBr injection (n = 6, mean ± SD).

dose range, the $T_{1/2}$ of Ani HBr remained consistent with the administration routes. The T_{max} showed minimal change with varying dosage, and there might be a dose-dependent relationship between C_{max} and the dosage.

In rats with LPS-induced septic ALI, we administered the same dosages and routes as in the physiological group. Based on the drug absorption, the disease state resulted in the T_{max} and C_{max} of Ani HBr tablets in rats exhibiting distinct features compared with the physiological group. As shown in Table 5, the T_{max} of Ani HBr in normal rats at 12.5, 25 and 50 mg/kg was 12.5 ± 9.9, 6.7 ± 4.1 and 12.0 ± 10.4 min, respectively, while the T_{max} in pathological conditions was significantly prolonged to 42.5 ± 27.5, 50.0 ± 24.5 and 25.0 ± 7.7 min. Concurrently, the C_{max} of the 12.5 mg/kg Ani HBr tablet-treated model group was notably reduced compared with the physiological group (81.4 ± 25.0 vs 164.5 ± 38.5 ng/ml). Following oral administration of 25 and 50 mg/kg Ani HBr tablets, the C_{max} for model group and physiological group rats were (210.3 ± 59.2 vs 364.0 ± 148.1, 445.6 ± 71.7 vs 890.6 ± 313.9 ng/ml), respectively. The above results indicated that after oral administration, the absorption rate of Ani HBr tablets in diseased rats was slowed down. To investigate the absorption of Ani HBr in rats under different states, we evaluated the area under the concentration-time curve from 0 to 24 h (AUC_{0-t})

Table 5. Pharmacokinetic parameter of Ani HBr after intragastric administration and intravenous administration in normal and model rats (n = 6, mean ± SD).

The route of administration	Dose (mg/kg)	Group	$T_{1/2}$ (h)	C_{max} (ng/ml)	T_{max} (min)	AUC_{0-t} (h*ng/ml)	$AUC_{0-\infty}$ (h*ng/ml)	Vz (l/kg)	CL (ml/min/kg)	MRT_{0-t} (h)
i.g.	12.5	N	3.0 ± 1.1	164.5 ± 38.5	12.5 ± 9.9	733.8 ± 371.0	1262.8 ± 796.9	6.2 ± 1.5	68.5 ± 6.5	4.5 ± 0.5
i.g.	12.5	M	6.1 ± 1.2[b]	81.4 ± 25.0[b]	42.5 ± 27.5[a]	416.2 ± 79.8	446.7 ± 84.4	6.6 ± 1.0	58.8 ± 10.9	8.9 ± 0.5[b]
i.g.	25	N	3.2 ± 0.6	364.0 ± 148.1	6.7 ± 4.1	937.4 ± 185.5	995.4 ± 229.9	9.2 ± 1.2	98.9 ± 5.9	4.6 ± 0.9
i.g.	25	M	7.0 ± 1.1[b]	210.3 ± 59.2[a]	50.0 ± 24.5[b]	1075.3 ± 259.7	1361.0 ± 392.7	9.8 ± 0.5	104.6 ± 3.0	7.2 ± 1.2[b]
i.g.	50	N	3.4 ± 1.2	890.6 ± 313.9	12.0 ± 10.4	1623.4 ± 381.6	1693.0 ± 383.6	9.2 ± 1.8	95.9 ± 4.9	4.3 ± 1.2
i.g.	50	M	6.8 ± 1.8[b]	445.6 ± 71.7[a]	25.0 ± 7.7[b]	3065.5 ± 1499.8[b]	6189.1 ± 4726.7[b]	15.0 ± 2.1[b]	60.8 ± 4.6[b]	9.1 ± 2.2[b]
i.v.	4	N	2.8 ± 0.3	1736.6 ± 453.5	2.0 ± 0.0	1119.5 ± 241.8	1125.2 ± 243.6	5.3 ± 1.4	61.5 ± 13.0	3.9 ± 0.8
i.v.	4	M	7.6 ± 1.4[b]	2336.6 ± 268.1[a]	2.0 ± 0.0	2432.3 ± 235.8[b]	2466.8 ± 239.8[b]	8.6 ± 3.0	27.2 ± 2.8[b]	6.8 ± 0.6[b]
i.v.	8	N	3.3 ± 0.5	3550.0 ± 388.4	2.0 ± 0.0	1774.7 ± 282.8	1781.9 ± 285.7	8.2 ± 2.2	76.2 ± 10.6	4.4 ± 0.2
i.v.	8	M	7.4 ± 0.7[b]	4128.3 ± 386.6[a]	2.0 ± 0.0	3953.6 ± 623.1[b]	4078.1 ± 751.8[b]	8.4 ± 1.5	33.5 ± 5.8[b]	8.2 ± 0.9[b]
i.v.	16	N	2.8 ± 0.4	5750.0 ± 511.8	2.0 ± 0.0	2751.3 ± 264.4	2759.4 ± 265.5	9.6 ± 2.1	97.4 ± 9.4	4.5 ± 0.2
i.v.	16	M	8.0 ± 0.9[b]	8456.7 ± 360.4[b]	2.0 ± 0.0	5848.5 ± 2519.2[a]	5904.8 ± 2528.6[a]	17.3 ± 6.6[a]	51.2 ± 18.1[b]	7.3 ± 1.0[b]

[a] $p < 0.05$.

[b] $p < 0.01$ compared with normal rats treated with the same dose at the same route of administration.

AUC_{0-t}: Area under the concentration-time curve from 0 to 24 h; $AUC_{0-\infty}$: Area under the concentration-time curve from 0 to time infinite; CL: Clearance rate; C_{max}: Maximum value of concentration; MRT_{0-t}: Mean residence time from 0 to 24 h; $T_{1/2}$P: Half-life of elimination; T_{max}: The time to achieve maximum concentration; V_z: Volume of distribution.

and area under the concentration-time curve from 0 to time infinite ($AUC_{0-\infty}$). However, we found that only after administration at a dose of 50 mg/kg, the AUC_{0-t} and $AUC_{0-\infty}$ in the model group were 3065.5 ± 1499.8 and 6189.1 ± 4726.7 h*ng/ml, respectively, while those in the physiological group were 1623.4 ± 381.6 and 1693.0 ± 383.6 h*ng/ml, significantly higher than the average level in the physiological group, indicating that Ani HBr has a higher absorption level in rats with sepsis-induced ALI at this dose, which is more conducive to the exertion of its efficacy. In addition, the volume of distribution (Vz) of the model group at this dose was significantly higher than that of the physiological group ($p < 0.01$), indicating that Ani HBr had a more extensive distribution in the model rats.

During the elimination of Ani HBr, after oral administration of 12.5 mg/kg Ani HBr tablets, the $T_{1/2}$ was extended from 3.0 ± 1.1 h in the physiological group to 6.1 ± 1.2 h in rats with ALI. Similarly, after i.g. of 25 and 50 mg/kg Ani HBr tablets, the $T_{1/2}$ of the model rats extended to 7.0 ± 1.1 and 6.8 ± 1.8 h, respectively, compared with 3.2 ± 0.6 and 3.4 ± 1.2 h in the physiological group, indicating a slower elimination of Ani HBr in the model rats. Correspondingly, the mean residence time from 0 to 24 h (MRT_{0-t}) also confirmed this fact. After being administered with 12.5 mg/kg Ani HBr tablets orally, the MRT_{0-t} of rats in the physiological group was 4.5 ± 0.5 h. However, the MRT_{0-t} of rats with LPS-induced septic ALI prolonged to 8.9 ± 0.5 h, which was approximately twice as long as that of the physiological group. After administering a higher dose, the MRT_{0-t} was delayed from 4.6 ± 0.9 to 7.2 ± 1.2 h at 25 mg/kg, and from 4.3 ± 1.2 to 9.1 ± 2.2 h at 50 mg/kg. The aforementioned results indicated that, at the identical dosage, Ani HBr took a longer time to accumulate within the body of rats with sepsis-induced ALI compared with normal rats.

The absorption of drugs is crucial for their efficacy. However, the absorption of Ani HBr in model rats was slow after i.g. Therefore, we also evaluated the pharmacokinetic characteristics of Ani HBr injection administered intravenously in model rats. The tail vein injection delivers drug directly into the blood circulation without the process of absorption, which makes Ani HBr take effect faster, and this is a major advantage of tail vein injection. As shown in Figure 5 & Table 5, at a dose of 4 mg/kg, the C_{max} in the model group was 2336.6 ± 268.1 ng/ml, which was higher than that of the physiological group 1736.6 ± 453.5 ng/ml ($p < 0.05$). The C_{max} of the model group at doses of 8 and 16 mg/kg was 4128.3 ± 386.6 and 8456.7 ± 360.4 ng/ml, respectively, and that of the normal group was 3550.0 ± 388.4 and 5750.0 ± 511.8 ng/ml, respectively, both significantly higher than those of the normal group. The phenomenon could be attributed to the slowed metabolism in pathological rats, which, coupled with systemic vascular microcirculation abnormalities, reduced the blood circulation speed and thereby lowered the elimination rate of Ani HBr in the bloodstream [18]. Given that Ani HBr entered the systemic circulation promptly after i.v., the T_{max} for each group occured within 2 min. In terms of AUC_{0-t} and $AUC_{0-\infty}$, the parameters for the model group exceeded those of the physiological group, suggesting that the exposure of Ani HBr in the blood is greater under pathological conditions than under physiological conditions.

The widespread distribution of medicines lays the foundation for their full efficacy. After i.v. of 4 and 8 mg/kg Ani HBr injection, we did not observe significant differences in Vz between the physiological group and the model group. However, after i.v. of 16 mg/kg Ani HBr injection, the results showed that the Vz of the model group was 17.3 ± 6.6 l/kg, which was significantly higher than that of the physiological group at 9.6 ± 2.1 l/kg, indicating that Ani HBr had a more extensive distribution in rats with septic ALI at this dose. In terms of drug clearance rate (CL), after i.v. of 4 mg/kg Ani HBr injection, the pathological group had a CL of 27.2 ± 2.8 ml/min/kg, which was significantly lower than that of the physiological group (61.5 ± 13.0 ml/min/kg). Similarly, after increasing the dose to 16 mg/kg, the CL of the model group remained significantly lower than that of the physiological group, indicating that the clearance of Ani HBr slowed down in septic rats. In line with this, following i.v. injection of 4, 8 and 16 mg/kg Ani HBr, the MRT_{0-t} in the model group was approximately 1.7, 1.8 and 1.6-times greater than that in the physiological group, suggesting a prolonged retention and slower metabolism of Ani HBr in rats with sepsis-induced ALI. Hence, it also accounted for the significantly higher C_{max} in the model group compared with the physiological group at the same dose.

4. Disscusion

Ani HBr is a highly polar tropane alkaloid [19]. We found that when using protein precipitation, the matrix can seriously interfere with its quantification, so we adopted a liquid-liquid extraction method and added NaOH to improve its recovery rate. Since the concentration of the drug in rat plasma decreases over time, a sensitive analytical method is needed for detection, so we used LC-MS/MS technology to evaluate the plasma pharmacokinetics of rats [20].

The pharmacokinetics of Ani have been investigated in human subjects, as well as in healthy mice, rats and beagle dogs. Ma et al. utilized micellar liquid chromatography to determine the pharmacokinetic characteristics of Ani after intramuscular administration in healthy humans,

with T_{max} observed at approximately 1 h [21]. In early preclinical studies, it was found that Ani was rapidly distributed in healthy mice after intraperitoneal injection and had $T_{1/2}$ of 2.9 h [22]. The pharmacokinetic characteristics of Ani in rats were investigated by Ma et al. using the LC-MS method. It was observed that the $T_{1/2}$ following oral administration of 60 mg/kg Ani in rats was determined to be 2.555 h, while AUC_{0-t} was found to be 1.992 h*μg/l [23]. Tian et al. conducted a pharmacokinetic study on Ani in healthy rats, administering it orally at a dose of 25 mg/kg and intravenously via the tail vein at a dose of 8 mg/kg. The results showed that T_{max} was observed at 0.56 $\pm$ 0.13 h after oral administration, with no significant difference in $T_{1/2}$ between the two routes of administration [17]. Additionally, Zhang et al. observed that the administration of *hyoscyamus niger* extract to rats via gavage resulted in T_{max} of Ani at 0.23 $\pm$ 0.29 h and $T_{1/2}$ of 3.34 $\pm$ 1.79 h [16]. The $T_{1/2}$ of anisodamine hydrochloride injection in Beagle dogs was 1.29 $\pm$ 0.10 h, while the AUC_{0-t} was at 2992.87 $\pm$ 182.16 h*ng/ml [24]. The T_{max} in healthy rats following gastric administration of Ani HBr tablets was observed to be within 0.5 h, indicating rapid systemic absorption, which is consistent with previous literature findings. Additionally, a comprehensive analysis of the pharmacokinetics of racemic anisodamine enantiomers in rabbits revealed that both the levorotatory and dextrorotatory forms exhibit analogous pharmacokinetic characteristics [25]. However, the configuration of a drug plays a pivotal role in determining its efficacy. As the natural levorotatory form, Ani HBr exhibits twice the binding affinity to M-choline receptors compared with its racemic counterpart, resulting in pharmacological activity that is 100–1000-times higher than that of the dextrorotatory form [6,26,27]. The application value of Ani HBr is higher, thus indicating its greater potential in clinical use.

The clearance of Ani primarily occurs in the rat intestinal flora through dehydration and hydrolysis, although its metabolic intensity is weak, predominantly existing as the parent drug [28]. However, Ani undergoes biotransformation in rat plasma, leading to six metabolites [29]. Our previous study found that the major hepatic metabolites of dehydrated anisodamine can still be detected after administration for 24 h, exhibiting non-linear kinetic characteristics [30,31]. It should be noted that the hydrolysis product of Ani, tropic acid, exhibits mutagenicity and thus poses potential risks to the safety of Ani HBr [32]. Zhu et al. developed an LC-MS/MS analysis method for tropic acid in rat plasma; however, there is still a dearth of simultaneous measurement of plasma concentrations for both of them [33]. Additionally, the Ani and seven phase I metabolites, along with four phase II metabolites, can be detected in rat urine. Similarly, it is excreted in feces as both the parent drug and phase I metabolites, indicating that Ani undergoes clearance via hepatic, renal and biliary pathways [34,35]. The important thing is that sepsis will downregulate the activity of liver CYP enzymes and decrease glomerular filtration rate, both of which will affect the clearance of Ani [36–38]. Therefore, our study provides a basis for the clinical application of Ani HBr tablets and injection in pathological conditions.

The alterations in the pharmacokinetic properties of Ani HBr may be associated with the intestinal microenvironment and vascular microcirculation in rats with pathological conditions [39]. Under physiological conditions, on the one hand, multipotent intestinal stem cells located at the bottom of small intestinal crypts can continuously proliferate and differentiate into absorptive small intestinal epithelial cells. In sepsis, proliferation and differentiation are suppressed, potentially resulting in a decrease in the number of absorptive small intestinal epithelial cells [40]. Furthermore, sepsis will hasten the apoptosis of intestinal epithelial cells, compromising the intestinal barrier [40–42]. On the other hand, sepsis causes widespread disturbances in the vascular microcirculation within the body, ultimately affecting systemic hemodynamics [2]. In the early stage of sepsis, the massive release of inflammatory factors encourages the adhesion of neutrophils to endothelial cells, activates coagulation factors and induces vascular fibrin deposition, ultimately leading to the formation of vascular microthrombi [41,43]. The intestinal mucosal layer and hepatic portal vein, as crucial regions for blood supply, will experience a reduction in blood flow due to mesenteric artery constriction during the onset of sepsis, potentially impacting drug absorption [44,45]. These may be the reasons for the weakened absorption of Ani HBr in septic rats. Similarly, the alterations in hemodynamics observed in sepsis will also result in impairments of liver and kidney function, leading to a decelerated clearance and prolonged retention time of Ani HBr [46,47].

Therefore, intravascular administration is a better way to treat the disease, which avoids absorption reduction, repair vascular damage and improve vascular microcirculation.

5. Conclusion

In this paper, we pioneered the establishment of a biosample analysis method for Ani HBr in rat plasma, based on LC-MS/MS technology, exhibiting strong specificity. The value exceeded 0.99 for concentrations ranging from 2 to 1000 ng/ml, with an accuracy range of 98.00–107.14% and a precision range of 3.91–10.44%. The extraction recovery rate of Ani HBr in rat plasma surpassed 89%, with no notable matrix interference. Subsequently, for the first time, we identified the differences in the pharma-

cokinetic characteristics of Ani HBr in rats under physiological and pathological conditions. Following a single gavage of LPS-induced septic ALI rats treated with 12.5, 25 and 50 mg/kg Ani HBr tablets, the C_{max} were significantly lower than that of the physiological group, while T_{max} were significantly prolonged. At a dose of 50 mg/kg, the AUC_{0-t} and $AUC_{0-\infty}$ values were 3065.5 ± 1499.8 and 6189.1 ± 4726.7 h*ng/ml, respectively, indicating significant differences compared with the physiological group. After a single tail vein injection of 4, 8 and 16 mg/kg Ani HBr injection to the model rats, due to the slowed metabolism, C_{max}, AUC_{0-t} and $AUC_{0-\infty}$ were higher than those of the physiological group, which would help to exert the drug effect. The above findings provide valuable experience for the development and application of Ani HBr and will contribute to a more comprehensive understanding of it.

Article highlights

- The alkaloid Ani HBr is derived from *Anisodus tanguticus* (Maxim.) Pascher in western China and possesses the ability to enhance vascular microcirculation disorders. Consequently, it has gained widespread recognition for its efficacy in treating septic shock.
- A sensitive and rapid LC-MS/MS method was first established and validated to explore the pharmacokinetic characteristics of Ani HBr tablets and injection in normal and septic acute lung injury rats.
- Under physiological conditions, Ani HBr tablets were rapidly absorbed into the bloodstream with T_{max} within 0.5 h. After oral and intravenous administration, $T_{1/2}$ was approximately 3 h, showing linear pharmacokinetic characteristics.
- In pathological conditions, the absorption of Ani HBr tablets was slowed down in rats with septic acute lung injury. However, after administration of the injection, the AUC significantly increased, $T_{1/2}$ and MRT were prolonged, which was more conducive to the exertion of pharmacological effects.

Author contributions

R Wu and Y Li conducted the experiments. R Wu and F Zhang wrote the manuscript and prepared the figures and tables. R Wu, F Zhang, Y Liu, X Yu, J Zhang, C Yao, S Dai and F Wan prepared material, collected the sample and analyzed the data. F Nan conceived the study.

Financial disclosure

This study was supported by the National Natural Science Foundation of China [grant number: 81891012, 81630101 and U19A2010], Sichuan Province Science and Technology Support Program [grant number: 2021JDRC0041, 2022ZYD0088], Innovation Team and Talents Cultivation Program of National Administration of Traditional Chinese Medicine [grant number: ZYYCXTD-D-202209], Sichuan TCM Science and Technology Industry Innovation Team [grant number: 2022C001]. The authors have no other relevant affiliations or financial involvement with any organization or entity with a financial interest in or financial conflict with the subject matter or materials discussed in the manuscript apart from those disclosed.

Competing interests disclosure

The authors have no competing interests or relevant affiliations with any organization or entity with the subject matter or materials discussed in the manuscript. This includes employment, consultancies, stock ownership or options and expert testimony.

Writing disclosure

No writing assistance was utilized in the production of this manuscript.

ORCID

Yunxia Li https://orcid.org/0000-0002-9256-5716

References

Papers of special note have been highlighted as: • of interest; •• of considerable interest

1. Van der Poll T, van de Veerdonk FL, Scicluna BP, et al. The immunopathology of sepsis and potential therapeutic targets. Nat Rev Immunol. 2017;17(7):407–420. doi:10.1038/nri.2017.36
2. Cecconi M, Evans L, Levy M, et al. Sepsis and septic shock. Lancet. 2018;392(10141):75–87. doi:10.1016/S0140-6736(18)30696-2
3. Rudd KE, Johnson SC, Agesa KM, et al. Global, regional, and national sepsis incidence and mortality, 1990-2017: analysis for the Global Burden of Disease Study. Lancet. 2020;395(10219):200–211. doi:10.1016/S0140-6736(19)32989-7
4. Qiu Y, Ouyang Z, Zhong J, et al. Anisodamine hydrobromide attenuates oxidative stress and proinflammatory cytokines in septic rats induced by cecal ligation and puncture. Cell. Mol. Biol. 2022;68(12):54–60. doi:10.14715/cmb/2022.68.12.11
5. Zhang Y, Zou J, Wan F, et al. Update on the sources, pharmacokinetics, pharmacological action, and clinical application of anisodamine. Biomed Pharmacother. 2023;161:114522. doi:10.1016/j.biopha.2023.114522
•• Shows an integrated review of the research progress on Ani HBr.
6. Zhang B, Luo L, Zhang X, et al. Research progress of anisodamine hydrobromide in the treatment of sepsis /septic shock. Pract Pharmacy Clin Remedies. 2022;25(10):934–938.
7. Zhong J, Ouyang Z, Shen J, et al. Improvement of hemodynamics in mesenteric microcirculation in septic shock rats by anisodamine and anisodine. Mechanobiol Med. 2023;1(1):100006–1000015. doi:10.1016/j.mbm.2023.100006
•• Shows pharmacological mechanisms underlying the efficacy of Ani in ameliorating vascular microcirculation disorders.
8. Zhang D, Mei X, Zhang F. A case report of septic shock patients treated with anisodamine hydrobromide injection. Chin Foreign Med Res. 2021;19(5):146–151.
9. Xu R, Li G. Clinical effect of anisodamine hydrobromide injection on improving microcirculation disturbance in elderly patients with abdominal pain. J Med Inform. 2022;35(19):124–126.

10. Lu J, Ji Q, Guo T. Effects of anisodamine hydrobromide on microcirculation and coronary endothelial function in patients undergoing cardiopulmonary resuscitation for cardiac arrest. China J Emerg Resuscitation Disaster Med. 2022;17(7):856–859.
11. Wan F, Chen K, Chen F, et al. Treatment of COVID-19 patients with anisodamine hydrobromide: three cases report and literature review. Front Med Sci Res. 2023;5(8):1–6. doi:10.25236/FMSR.2023.050801
    •• **Shows the benefits of Ani HBr in clinical applications.**
12. De Backer D, Ricottilli F, Ospina-Tascon GA. Septic shock: a microcirculation disease. Curr Opin Anaesthesiol. 2021;34(2):85–91. doi:10.1097/ACO.0000000000000957
13. Beach JM, McGahren ED, Duling BR. Capillaries and arterioles are electrically coupled in hamster cheek pouch. Am. J. Physiol. 1998;275(4):H1489–1496. doi:10.1152/ajpheart.1998.275.4.H1489
14. Ren X, Wang Z, Wang X, et al. Determination of aloesone in rat plasma by LC-MS/MS spectrometry and its application in a pharmacokinetic study. Bioanalysis. 2024;16(10):453–460. doi:10.4155/bio-2023-0231
15. Zhu Y, Fan Y, Cao X, et al. Pharmacokinetic-pharmacodynamic (PK/PD) modeling to study the hepatoprotective effect of Perilla Folium on the acute hepatic injury rats. J Ethnopharmacol. 2023;313:116589. doi:10.1016/j.jep.2023.116589
16. Zhang P, Li Y, Liu G, et al. Simultaneous determination of atropine, scopolamine, and anisodamine from Hyoscyamus niger L. in rat plasma by high-performance liquid chromatography with tandem mass spectrometry and its application to a pharmacokinetics study. J Sep Sci. 2014;37(19):2664–2674. doi:10.1002/jssc.201400534
17. Tian F, Li C, Wang X, et al. Comparative study on pharmacokinetics of a series of anticholinergics, atropine, anisodamine, anisodine, scopolamine and tiotropium in rats. Eur J Drug Metab Pharmacokinet. 2015;40(3):245–253. doi:10.1007/s13318-014-0192-y
    • **Shows pharmacokinetic characteristics of tropane alkaloids in healthy rats.**
18. Su J, Coleman P, Ntorla A, et al. Sensing cytosolic DNA lowers blood pressure by direct cGAMP-dependent PKGI activation. Circulation. 2023;148(13):1023–1034. doi:10.1161/CIRCULATIONAHA.123.065547
19. Wang PY, Chen JW, Hwang F. Anisodamine causes acyl chain interdigitation in phosphatidylglycerol. FEBS Lett. 1993;332(1–2):193–196. doi:10.1016/0014-5793(93)80511-R
20. Chen R, Ning Z, Zheng C, et al. Simultaneous determination of 16 alkaloids in blood by ultrahigh-performance liquid chromatography-tandem mass spectrometry coupled with supported liquid extraction. J Chromatogr B Analyt Technol Biomed Life Sci. 2019;1128:121789. doi:10.1016/j.jchromb.2019.121789
21. Ma P, Wu C. Determination of blood concentration and pharmacokinetic parameters of anisodamine by micellar liquid chromatography. Acta Pharmaceutica Sinica. 1992;(10):763–767.
22. Zhan L, Zhang Y, He M. Determination of apparent pharmacokinetic parameters of anisodamine by acute mortality of mice. Chin J Pharmacol Toxicol. 1987;3(1):224–228.
23. Ma X, Wang X, Chen Y, et al. Determination of anisodamine in plasma of rat by HPLC-MS. Chin Trad Herb Drugs. 2008;39(9):1312–1315.
24. Li W, Wen J, He J, et al. Development and validation of a rapid and sensitive assay for the determination of anisodamine in 50 muL of beagle dog plasma by LC-MS/MS. J Sep Sci. 2013;36(19):3184–3190. doi:10.1002/jssc.201300451
25. Fan GR, Hong ZY, Lin M, et al. Study of stereoselective pharmacokinetics of anisodamine enantiomers in rabbits by capillary electrophoresis. J Chromatogr B Analyt Technol Biomed Life Sci. 2004;809(2):265–271. doi:10.1016/S1570-0232(04)00510-0
26. Niu X, Ren Z, Xie L. Potencies of four stereoisomers of anisodamine on muscarinic receptor. J Chin Pharm Sci. 1992;(02):86 + 84–85.
27. Zeng Y, Qiu Y, Jiang W, et al. Research progress on the mechanism of anisodamine hydrobromide in improving microcirculation disorders. J Jiangsu University. 2021;31(01):23–27.
28. Chen H, Du P, Han F, et al. Analysis of anisodamine and its *in vitro* metabolites in rat intestinal flora by LC-MSn. Chin Traditional Herb Drugs. 2009;40(4):563–565.
29. Chen Y, Du P, Han F, et al. Identification of anisodamine and its metabolites in rat plasma by liquid chromatography tandem mass spectrometry. Chin Pharm J. 2006;41(15):1178–1181.
    •• **Shows metabolic pathways and metabolite profiles of Ani in rat plasma.**
30. Wu R, Liu Y, Zhang F, et al. Study on pharmacokinetics of raceanisodamine impurityl in Rats by LC-MS/MS. Pharm Clin Chin Materia Medica. 2023;14(6):65–68.
31. Chen H, Chen Y. Analysis of anisodamine and its metabolites in homogenized liver of rat by liquid chromatography tandem mass spectrometry. J Hubei University. 2006;28(3):296–298.
32. Qu J, Chen D, Zhao Y, et al. Study on mutagenicity mechanism of tropic acid. China Pharm. 2014;25(9): 444–448. doi:10.1021/bc400530s
    • **Shows the potential hazards associated with tropic acid.**
33. Zhu G, Tong Z, Ping L. Determination of the concentration of tropine acid in rat plasma using ultra high performance liquid chromatography-tandem mass spectrometry. Chin J Anal Lab. 2021;40(4):444–448.
34. Chen H, Wang H, Chen Y, et al. Liquid chromatography-tandem mass spectrometry analysis of anisodamine and its phase I and II metabolites in rat urine. J Chromatogr B Analyt Technol Biomed Life Sci. 2005;824(1–2):21–29. doi:10.1016/j.jchromb.2005.07.036
35. Chen H, Du P, Han F, et al. Detection of anisodamine and its metabolites in rat feces by tandem mass spectromeetry. Acta Pharmaceutica Sinica. 2006;41(12):1166–1169.
36. Morgan ET. Regulation of cytochrome p450 by inflammatory mediators: why and how? Drug Metab Dispos. 2001;29(3):207–212. doi:10.1016/S0300-483X(02)00283-4
37. Harvey RD, Morgan ET. Cancer, inflammation, and therapy: effects on cytochrome p450-mediated drug metabolism and implications for novel immunothera-

peutic agents. Clin Pharmacol Ther. 2014;96(4):449–457. doi:10.1038/clpt.2014.143
38. Manrique-Caballero CL, Del Rio-Pertuz G, Gomez H. Sepsis-associated acute kidney injury. Crit Care Clin. 2021;37(2):279–301. doi:10.1016/j.ccc.2020.11.010
39. Rajaee A, Barnett R, Cheadle WG. Pathogen- and danger-associated molecular patterns and the cytokine response in sepsis. Surg Infect (Larchmt). 2018;19(2):107–116. doi:10.1089/sur.2017.264
40. Fay KT, Ford ML, Coopersmith CM. The intestinal microenvironment in sepsis. Biochim Biophys Acta Mol Basis Dis. 2017;1863(10 Pt B):2574–2583. doi:10.1016/j.bbadis.2017.03.005
41. Hotchkiss RS, Karl IE. The pathophysiology and treatment of sepsis. N Engl J Med. 2003;348(2):138–150. doi:10.1056/NEJMra021333
42. Hotchkiss RS, Swanson PE, Cobb JP, et al. Apoptosis in lymphoid and parenchymal cells during sepsis: findings in normal and T- and B-cell-deficient mice. Crit Care Med. 1997;25(8):1298–1307. doi:10.1097/00003246-199708000-00015
43. Simmons J, Pittet JF. The coagulopathy of acute sepsis. Curr Opin Anaesthesiol. 2015;28(2):227–236. doi:10.1097/ACO.0000000000000163
44. Wang XH, Xu DQ, Chen YY, et al. Traditional Chinese Medicine: a promising strategy to regulate inflammation, intestinal disorders and impaired immune function due to sepsis. Front Pharmacol. 2022;13:952938. doi:10.3389/fphar.2022.952938
45. Liu S, Kohler A, Langer R, et al. Hepatic blood flow regulation but not oxygen extraction capability is impaired in prolonged experimental abdominal sepsis. Am J Physiol Gastrointest Liver Physiol. 2022;323(4):G348–G361. doi:10.1152/ajpgi.00109.2022
46. Strnad P, Tacke F, Koch A, et al. Liver - guardian, modifier and target of sepsis. Nat Rev Gastroenterol Hepatol. 2017;14(1):55–66. doi:10.1038/nrgastro.2016.168
47. Peerapornratana S, Manrique-Caballero CL, Gomez H, et al. Acute kidney injury from sepsis: current concepts, epidemiology, pathophysiology, prevention and treatment. Kidney Int. 2019;96(5):1083–1099. doi:10.1016/j.kint.2019.05.026